COMPUTER-AIDED DESIGN & APPLICATIONS, 2018
VOL. 15, NO. 5, 643–652
https://doi.org/10.1080/16864360.2018.1441230



# Artificial intelligence aided CFD analysis regime validation and selection in feature-based cyclic CAD/CFD interaction process

Lei Li, Carlos F. Lange and Yongsheng Ma

University of Alberta, Canada

**ABSTRACT**

Multiple-view feature modeling is supposed to keep the information consistency during product development. However, for products involving fluid flow, the information consistency is difficult to keep because the application of CFD (Computational Fluid Dynamics) requires specific knowledge and rich experience. To conquer this deficiency, intelligent CFD solver functions toward an expert system are proposed to update the CFD analysis view in response to the changes in the design view which is embedded in the CAD fluid functional features. The CAE interface protocol is used to convert the features in the design view into the CAE boundary features in the CFD analysis view. The CFD analysis view also includes the fluid physics features and dynamic physics features which support the intelligent CFD solver functions. The intelligent CFD solver is enhanced with the capability to model complex turbulent phenomena and estimate the discretization error. A case study of contracted pipe is illustrated to show the effectiveness of the proposed multiple-view feature modeling method by comparing with empirical results.

**KEYWORDS**

CAD; CFD analysis view; multiple-view feature modeling; expert system

## 1. Introduction

With the development of feature modeling techniques, the application of features is not restricted to represent the generic shapes only. In the whole product lifecycle, features can also be used to model the non-geometric properties which are usually driven by different activities in product development [24]. Each activity has its own way of looking at a product [2]. However, excessive subjective decisions and manipulations exist in this process, which reduces the consistency and efficiency [19]. Multiple-view feature modeling provides a specific view for each product development phase and keeps the information consistency through view updating [4]. Specifically, for simulation-based design, the analysis view [26] should be fully integrated with CAD models in a multiple-view product development environment. In the development of fluid flow products, CFD (Computational Fluid Dynamics) technology is increasingly used as an advanced support. However, the successful application of CFD requires special knowledge and rich experience, which is a barrier for the conversion from the design view to the analysis view, and the maintenance of information consistency. So far, the integrated analysis view with CFD involvement has not been well studied.

There have been several approaches to multiple feature views, which take advantage of design by features, feature recognition [9] and feature conversion [3, 28]. Cunningham and Dixon [6] use design by features and feature conversion to create the feature model for the design view and the finite-element model for the analysis view, respectively [4]. Anderson and Chang [1] propose a geometric reasoning method called feature refinement to convert features in the design view into process planning procedures in manufacturing view for material removal operations. For injection moulding product, Deng et al. [10] propose CAD-CAE features to capture both geometric and non-geometric information from the design view, which are used to establish the analysis view. Lee [15] identifies the design view of the moulding product contains the form features and the mouldability features. Meanwhile, the manufacture view is focused on the design of the mould. The translation from the design view to the manufacture view is based on the geometric relationships between the product and the mould. Liu et al. [20] propose the associative optimization feature model to build the structural optimization view of the product.

The aforementioned approaches fall into the one-way feature conversion in which features are usually derived from the original design view [13]. Hoffmann and Joan-Arinyo [12] put forward a master model which has domain-specific clients who have their own view of the product model. The CAD view, geometric dimensioning

**CONTACT** Lei Li lli7@ualberta.ca; Carlos F. Lange carlos.lange@ualberta.ca; Yongsheng Ma yongsheng.ma@ualberta.ca

and tolerancing view, manufacturing process planning view and other downstream views can be coordinated by the master model under the control of the change protocol. Thus, multi-way feature conversion [8] is achieved and the consistency is maintained at the same time. Instead of focusing on the completely specified geometry and a single part, Bronsvoort and Noort [4] introduce a new multiple-view feature modeling approach which provides the conceptual design view, assembly design view, part detail design view and part manufacturing planning view. This approach not only supports the later phases of product development, but also the earlier phases. Thus, a designer is able to specify the product model from an arbitrary view, and the consistency is kept by automatic consistency checking and recovering algorithms.

Based on the multiple-view feature modeling approach, Smit and Bronsvoort [26] propose that the analysis view should be a feature model to propagate the changes in a multi-directional manner. However, the current CFD solver structure does not support this generally. It should be noted that incorporating knowledge in the analysis process is essential for the integration of analysis with other activities in product development [26]. Therefore, by applying artificial intelligence, CFD expert system can be used to capture the knowledge needed in CFD analysis and aid the automatic analysis regime validation and selection in response to the changes in the design view.

As an early attempt, Kutler and Mehta [14] investigate the potential impact of artificial intelligence on aerodynamic simulation. EXFAN, a cooling fan design system, is one of the first implemented AI/CFD systems [29]. EXFAN is a rule-based system which starts with a primary input and gradually modifies it through iterative CFD analysis till the satisfactory design is obtained. A hybrid system which incorporates both conventional and expert systems is established by Dannenhoffer and Baron [7] to conduct local compressible flow analysis. Aided by artificial intelligence, Shelton et al. [25] use a design shell coupled with a CFD solver to optimize the airfoil design. Rubio et al. [23] use artificial neural network to create an expert system which can be used to predict the time required for the convergence of a CFD problem. Wesley et al. [30] bring forward a CFD expert system by integrating AI and CFD to monitor the user input and inspect unreasonable combination of operations. To guide the CFD projects and aid the users in applying CFD, Stremel et al. [27] implement BPX (Best Practices eXpert). So far, the automated CFD solver functions are still urgently needed because the knowledge behind the solvers is still nontransparent to junior users.

In this paper, the CAE interface protocol [17] is used to convert the fluid functional features [18] in the design view into the CAE boundary features [17] in the CFD analysis view. Based on the physical knowledge, intelligent CFD solver functions toward an expert system are established to further process those features and generate a robust simulation model with the help of fluid physics features and dynamic physics features [18] in the CFD analysis view. Consequently, the consistency is kept properly and the CFD analysis view can be fully fulfilled. The following section introduces the mechanism of feature conversion between different views. The feature model of the CFD analysis view based on the intelligent CFD solver is described in Section 3. In addition, the subroutine for the advanced turbulence model and the process of grid independence analysis and error estimation are developed for this intelligent CFD solver. Section 4 demonstrates the case study of a section of a contracted pipe, which is used to show the functions of the proposed feature-based intelligent CFD solver and compare the results obtained from this system with empirical results. The conclusions are made at last.

## 2. Feature conversion

Based on the engineering knowledge, including properties, behaviors, shapes, and physical phenomena relating objects [5], and using design by features, the geometry of the product can be created parametrically. According to the functional requirement derived from design intent, the CAD fluid functional feature is defined as a class of design intent attributes which are composed of design parameters and functional descriptions, as well as functional fluid geometry [18]. The CAD fluid functional features not only convey the design intent to the downstream applications but also entail the design view. As a result, except for the geometrical features, the design view covers the non-geometrical features as well.

CFD is a numerical method to analyze the fluid flow problems. The solving space is usually a discretized fluid domain bounded by boundary conditions. The features in the design view are transformed into features in the CFD analysis view through feature conversion. To achieve this, the fluid domain needs to be abstracted with necessary defeaturing. Based on the function of the product, the non-geometrical features like design objective, fluid properties and boundary conditions can be derived from the design intent attributes. Such kind of information is stored in the database, which can be used in the CFD model. In order to keep the consistency, the faces of the fluid domain are assigned specific tags to identify their boundary type. The tag is an identifier which can be recognized by both CAD and CFD systems. It works as part of the CAE interface protocol. Tab. 1 shows the mechanism of the geometric feature

**Table 1.** Geometric information transmission in the feature conversion [17].

| Tag | Attribute | Boundary condition |
|---|---|---|
| $I_1, I_2, I_3, \ldots \ldots, I_m$ | Inlet | Velocity or pressure inlet |
| $O_1, O_2, O_3, \ldots \ldots, O_n$ | Outlet | Velocity or pressure outlet |
| $W_1, W_2, W_3, \ldots \ldots, W_p$ | Wall | No-slip wall |
| $S_1, S_2, S_3, \ldots \ldots, S_q$ | Symmetrical plane | Symmetry |

conversion between the design view and the CFD analysis view, in which m, n, p and q are the numbers of the corresponding faces in the abstracted fluid domain [17]. Then, the mesh can be generated based on the boundary type and the boundary conditions can be assigned, correspondingly. Ma et al. [21] suggest that the associative feature [22] can be used to establish the built-in links among the related application-specific features while feature consistency is kept by self-validation methods. As an extensive application of the associative feature, the CAE boundary features include the fluid attributes inherited from the design intent attributes and the meshed fluid domain with boundary conditions attached. Thus, the CAE boundary features link the CAD fluid functional features in the design view and the downstream fluid physics features to be introduced in the next section. This feature conversion process is depicted in Fig. 1.

## 3. Feature-based CFD analysis view

### 3.1. Feature model of the CFD analysis view

Different from the static analysis, the CFD model requires special expertise and rich experience to deal with the nonlinearity. Thus, the solver configuration is a time-consuming process and prone to mistakes, which may lead to inaccurate results. Here, we propose to develop

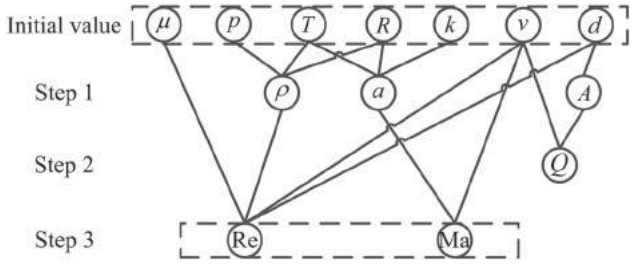


**Figure 2.** Data processing module.

intelligent CFD solver functions for dry steam simulation, which are composed of different modules.

The data processing module of the intelligent CFD solver is depicted in Fig. 2. The initial values are obtained from the fluid attributes which are stored in the database. The parameters in the following steps can be derived using equations [18]. Here, $\mu$ is the dynamic viscosity of gas, $p$ is the pressure of gas, $T$ is the temperature of gas, $R$ is the gas constant, $k$ is the specific heat ratio of gas, $v$ is the velocity of gas, $d$ is the inner diameter of duct, $\rho$ is the density of gas, $a$ is the speed of sound of gas, $A$ is the cross-sectional area of duct, $Q$ is the flow rate of gas, Re is the Reynolds number, and Ma is the Mach number. The Reynolds number and Mach number determine the flow regime, and they can always be obtained regardless of the occurrence order of the other parameters if the initial data pool is sufficient.

If the Reynolds number exceeds the critical value (4000 for flow in the pipe), a turbulence model will be selected. Meanwhile, the Mach number judges whether the flow is compressible. If the compressibility effects cannot be ignored (Ma $>$ 0.3), the total energy model should be selected and the reference pressure, as well as proper

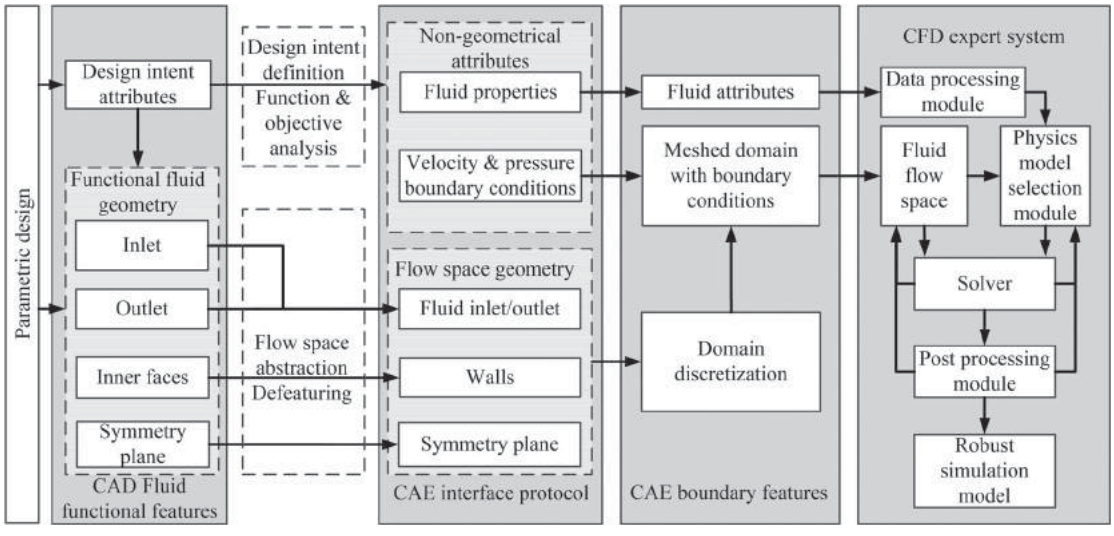


**Figure 1.** Feature conversion between the design view and the CFD analysis view.

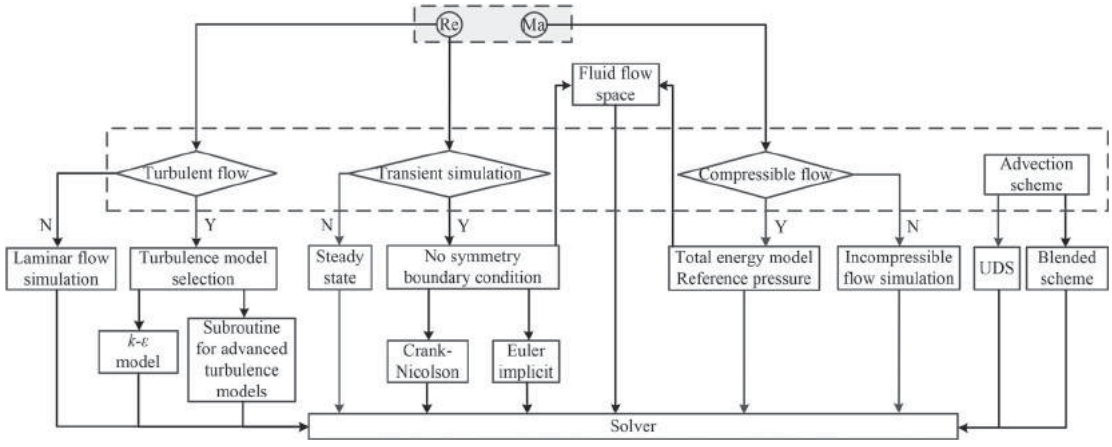


**Figure 3.** Physics model selection module.

boundary conditions should be setup to trigger the compressible flow simulation. In the preliminary stage of the simulation or at the time the simulation has convergence problems, lower order discretization schemes like UDS (Upwind Differencing Scheme) and Euler implicit, as well as $k-\varepsilon$ turbulence model if applicable, are preferred to assist convergence. This physics model selection process is illustrated in Fig. 3.

The residual is used as the convergence criteria of the solving process. As shown in Fig. 4, the index i (iteration), C (Convergence) and D (Divergence) will be updated after each simulation run. All the solver setup and the convergence status are recorded no matter whether the simulation is converged or not. If a simulation converged, post processing will be conducted to check whether the solution matches the initial assumptions and expected accuracy. If not, grid adaption will be activated based on the existing simulation result. According to the peak value of Reynolds number and Mach number obtained from the simulation, the flow regime is double checked to see whether the simulation model needs to be changed. If a simulation diverged, the solver setup should be modified to achieve convergence. It should be noted that each time when a new iteration starts, only one change is allowed in the solver configuration to obtain the sensitivity towards different simulation schemes. If the simulation still has convergence problems after several successive runs, human intervention is needed to diagnose the problem.

Higher order schemes can be applied after rounds of successful simulations because the mesh will be further refined. In such kind of situation, a subroutine will be entered to select one advanced turbulence model if the flow is turbulent. This program stops when the selected turbulence model is able to demonstrate the dominant features observed in the real-world turbulent flow based on the converged simulation. If the flow regime used to judge the fluid physics models is valid, grid independence analysis will be conducted to see whether the simulation is still affected by the grid refinement. By this analysis, the error of the discretization can be estimated if the grid is independent. The detailed description of the subroutine for advanced turbulence models and grid independence analysis will be introduced in subsection 3.2 and 3.3, respectively. Consequently, the accuracy of the final simulation can be guaranteed. During this process, the dynamic physics feature is developed to facilitate the generation of the robust simulation model [18].

In this system, the physical parameters are the component of the object oriented fluid physics feature which also embeds a set of rules to select the proper CFD solver regime. Therefore, the proposed system is a rule based system, and the CFD analysis view in this system is a feature based model which contains CAE boundary features, fluid physics features, and dynamic physics features. The knowledge of engineering, physics, and numerical method is applied in this CAD/CFD interaction process, which contributes to the smooth feature conversion and automation.

### 3.2. Subroutine for advanced turbulence models

There are several methods available to model the turbulence, such as RANS (Reynolds Averaged Navier-Stokes), LES (Large Eddy Simulation), and DNS (Direct Numerical Simulation). In DNS, the Navier-Stokes equations are solved for all the motions in a turbulent flow, which provides very detailed information of the flow. However, DNS is too computationally expensive making it hard to be a design tool. LES is good for transient large-scale fluctuating flows. Though less costly than DNS, LES is still computationally expensive because it is three

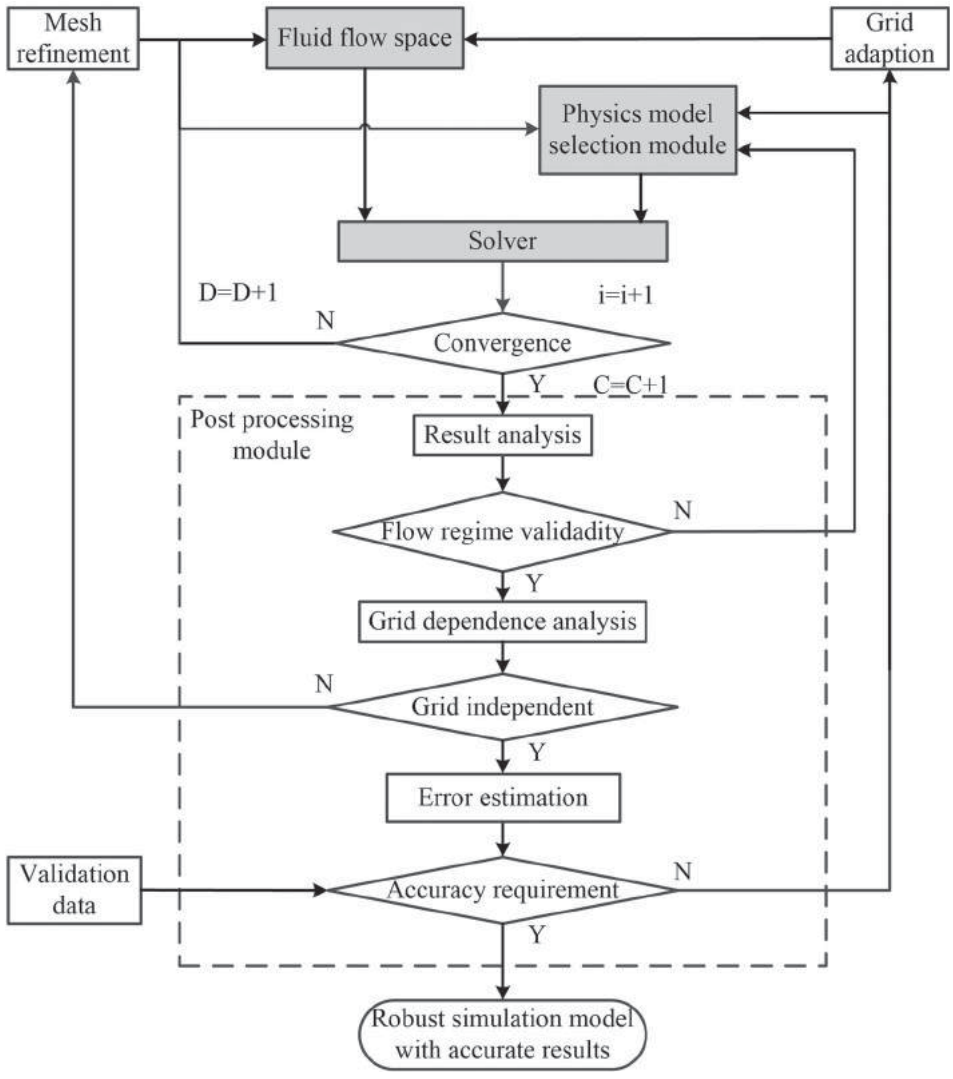


**Figure 4.** Post processing module.

dimensional and time dependent [11]. So the advanced turbulence models used in the subroutine focus on RANS models including $k-\omega$, RSM (Reynolds Stress Models), and SAS (Scale-Adaptive Simulation).

The structure of the subroutine for advanced turbulence models is shown in Fig. 5. When the subroutine for advanced turbulence models is entered, after an initial solution with the $k-\varepsilon$ model, the $k-\omega$ model will be selected first as the turbulence model. If it is not capable to model the turbulence accurately, RSM or SAS will be selected according to the flow regime obtained from the initial simulation result with $k-\varepsilon$ model. In both RSM and SAS, the $\Delta$t should be tested for step size independence before checking whether the selected turbulence model is acceptable. If the result is still not acceptable, the fluid physics models will be updated to achieve better cooperation with the turbulence model. If none of the models in the subroutine is applicable, $k-\varepsilon$ model will be reselected with updated fluid physics models.

### 3.3. Grid independence analysis and error estimation

In order to estimate the discretization error, grid independence analysis needs to be conducted first to see whether the solution will change fundamentally with the further refinement of the grid. 3 successively refined grids with different refinement levels are needed to conduct the grid independence analysis. If the characteristic parameter approaches the exact value asymptotically, then the order of discretization can be calculated. In this case, assume that the grid spacing of the coarse, medium, and fine mesh is $\Delta x_1$, $\Delta x_2$, and $\Delta x_3$, respectively, then the refinement rate $\alpha$ is:

$$\alpha = \frac{\Delta x_1}{\Delta x_2} = \frac{\Delta x_2}{\Delta x_3} \tag{3.1}$$

CFD uses discretized equations to approximate the differential equation. Usually, the exact solution $\phi(x)$ in

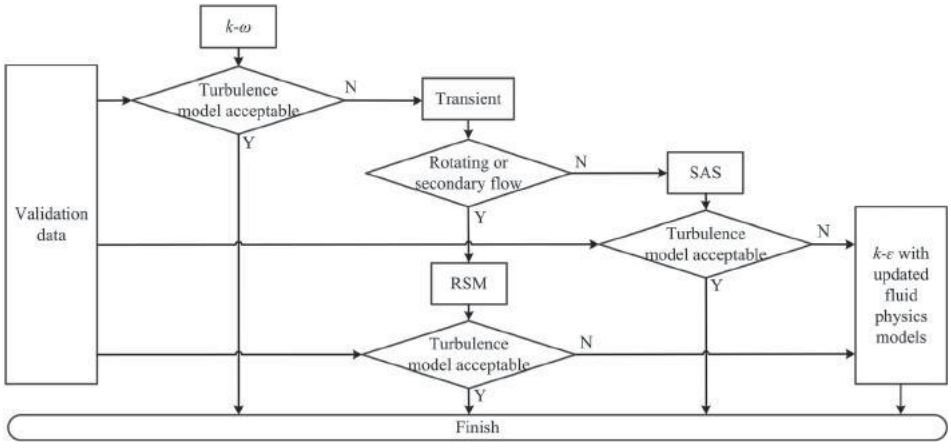


**Figure 5.** Subroutine for advanced turbulence models.

CFD simulation is not known. Incorporating the refinement rate calculated using Eqn. (3.1), the value of $\phi$ in each grid level is used to estimate the order $p$ of the discretization scheme:

$$p \approx \frac{\log\left(\frac{\phi_{\Delta x_2}-\phi_{\Delta x_1}}{\phi_{\Delta x_3}-\phi_{\Delta x_2}}\right)}{\log(\alpha)} \tag{3.2}$$

Grid independence can be claimed if $p$ is close to 2 for 2nd order discretization schemes or between 0.8 to 2.2 for a combination of 1st and 2nd order discretization schemes. Neither negative nor very large $p$ values can be accepted as grid independence. By Richardson extrapolation [11], the discretization error $\varepsilon_h^d$ can be estimated using Eqn. (3.3) and a better approximation of the exact value can be found:

$$\varepsilon_h^d = \frac{f_{\Delta x_3} - f_{\Delta x_2}}{\alpha^p - 1} \tag{3.3}$$

$$\phi_{exact} \approx \phi_{\Delta x_3} + \varepsilon_h^d \tag{3.4}$$

Typically, in the grid independence analysis, an integral parameter, which is relevant and sensitive to the entire flow field, should be chosen as the characteristic parameter $\phi(x)$. Because the grid independence can be expected only on sufficiently fine grids, the mesh needs to be refined further if the grid independent solution is not reached. If the accuracy of the simulation is not acceptable, grid adaption will be conducted and the physical models will be adjusted to achieve better results.

## 4. Case study

### 4.1. Design and analysis of contracted pipe

Fig. 6(a) shows a section of a pipe with a contraction which induces flow separation and mixing. The design and analysis of the piping system are selected as the case study. The reason is that the pressure drop under a certain flow rate in the piping system can be determined by head loss calculation [32], and it can be used as a benchmark for the simulation results. The fluid domain is created by feature conversion and is shown in Fig. 6(b). Under the control of CAE boundary features, the mesh is generated as shown in Fig. 6(c). The initial value of the design parameter $d$ (small inner diameter of the pipe) in this sample case is 70 mm.

At the inlet of the fluid domain, dry steam flows at 1 m/s. The pressure of 101325 Pa is assigned to the outlet. The other initial physical parameters are collected in Tab. 2. Using equations, the physical parameters in Tab. 3 are derived. The flow rate is calculated to be 0.031 $m^3/s$ in step 2. The Reynolds number and Mach number are 9561 and 0.002, respectively. Therefore, the flow is assumed to be incompressible turbulent flow. Then the physics models are selected accordingly by the intelligent CFD

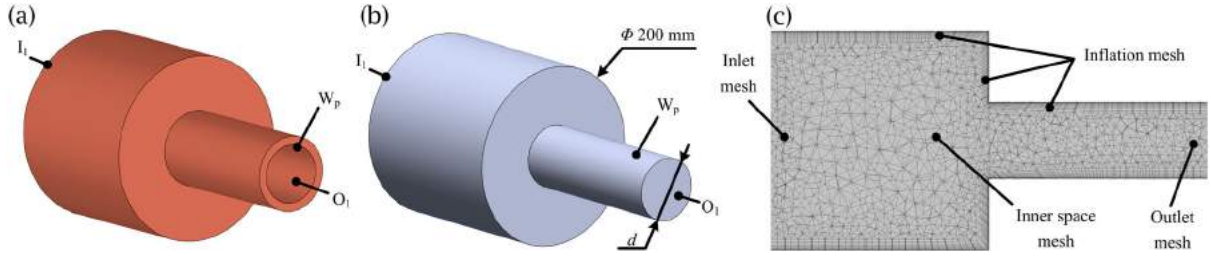


**Figure 6.** Model conversion in the pipe analysis: (a) Contracted pipe, (b) Fluid domain, (c) Mesh generation.

**Table 2.** The initial values of the physical parameters.

| Physical parameter | Value | Unit |
|---|---|---|
| $\mu$ | $1.23\times10^{-5}$ | kg/(m s) |
| $p$ | $1.013\times10^{5}$ | Pa |
| $T$ | 373.15 | K |
| $R$ | 461.5 | J/(kg K) |
| $k$ | 1.327 | N/A |
| $v$ | 1 | m/s |
| $d$ | 0.2 | m |

**Table 3.** The values of physical parameters calculated in step 1.

| Physical parameter | Value | Unit |
|---|---|---|
| $\rho$ | 0.588 | $kg/m^3$ |
| $a$ | 478 | m/s |
| $A$ | 0.031 | $m^2$ |

solver. The mesh generated by adaptive method is shown in Fig. 7(a). To conduct the grid independence analysis, this grid is systematically refined at the rate of 1.1. Based on those 3 grids and the physics models, the simulation is conducted. In the analysis of pipe flow, one of the important quantities is the pressure drop. The number of nodes and the value of pressure drop corresponding to each refinement level are tabulated in Tab. 4. The pressure drop is selected as the characteristic parameter and its trend

**Table 4.** Pressure drop calculation based on different grids.

| Refinement level | Numberof nodes | $\Delta p$ (Pa) |
|---|---|---|
| Coarse (original mesh) | 83414 | 30.62 |
| Medium | 109238 | 30.381 |
| Fine | 144429 | 30.181 |

towards the number of nodes is depicted in Fig. 7(b). Apparently, all the pressure drops are in the asymptotic region of the solution space. By Eqn. (3.2), the order $p$ is calculated to be 1.87. Because the blended scheme is applied as the advection scheme, which corresponds to a weighted average between UDS and CDS (Central Differencing Scheme), the calculated $p$ value corresponds to the discretization scheme used. Therefore, grid independence is achieved. Using Eqn. (3.3) and Eqn. (3.4), the discretization error and the approximated exact solution is found to be -1.025 and 29.156, respectively. The pressure and velocity vectors obtained from the robust simulation model are shown in Fig. 8.

### 4.2. Result comparison between different designs

With the design parameter $d$ decreasing, the pressure drop between the inlet and outlet is tabulated in Tab. 5.

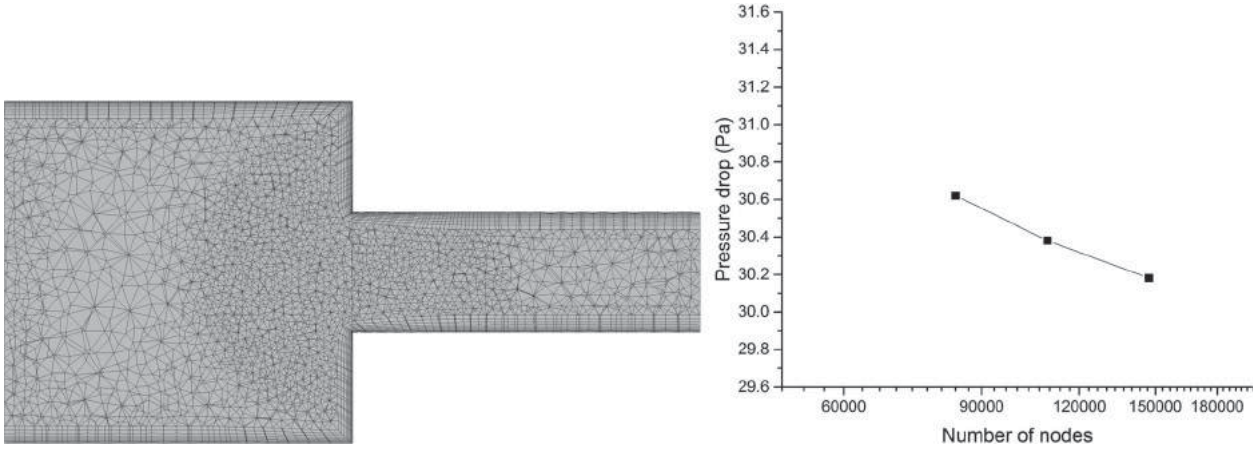


**Figure 7.** Mesh generation and assessment: (a) Adaptively refined mesh, (b) Grid independence analysis.

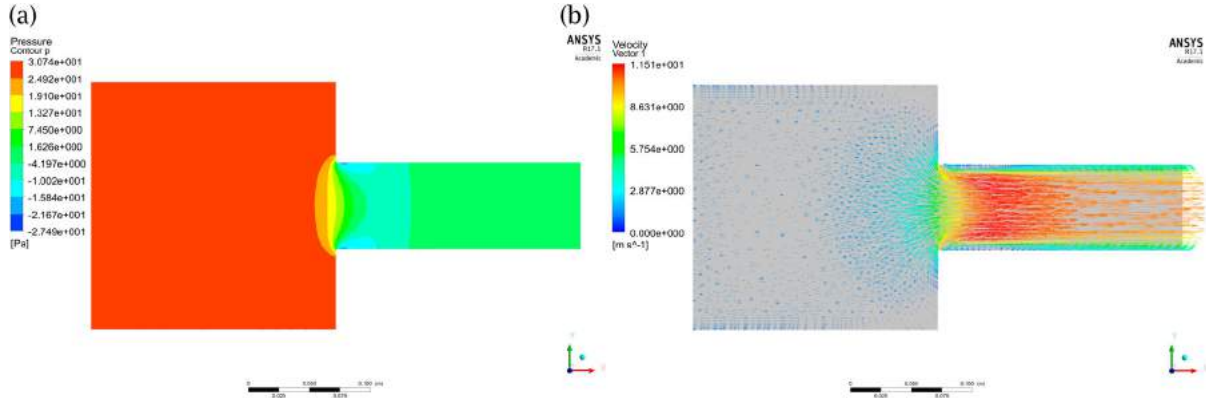


**Figure 8.** Results obtained from the robust simulation model: (a) Pressure contour, (b) Velocity vectors.

**Table 5.** Pressure drop calculation based on different methods.

| Design point | $d$ (mm) | $\Delta p$ (Pa) | $\Delta p_1$ (Pa) | $\delta_1$(%) | No. of nodes in batch mode | $\Delta p_2$ (Pa) | $\delta_2$(%) | No. of nodes in intelligent system |
|---|---|---|---|---|---|---|---|---|
| DP1 | 70 | 29.05 | 32.18 | 10.77 | 59297 | 30.62 | 5.40 | 83414 |
| DP2 | 60 | 54.32 | 60.81 | 11.94 | 57853 | 57.39 | 5.65 | 80573 |
| DP3 | 50 | 113.45 | 129.64 | 14.27 | 56296 | 120.04 | 5.81 | 77486 |
| DP4 | 40 | 278.35 | 325.01 | 16.76 | 56220 | 296.57 | 6.55 | 76353 |
| DP5 | 30 | 882.52 | 1065.67 | 20.75 | 59466 | 959.09 | 8.68 | 76235 |
| DP6 | 20 | 4478.13 | 6156.05 | 37.46 | 65952 | 5057.10 | 12.93 | 78895 |

**Table 6.** Physics models selected for the batch mode.

| Physics models in batch mode | Selection |
|---|---|
| Turbulence model | $k$-$\epsilon$ |
| Advection scheme | UDS |
| Transient model | No |
| Compressible flow model | No |

**Table 7.** Physics models selected for the first round of simulation of design point 6.

| Physics models in intelligent system(i = 1; C = 1; D = 0) | Selection |
|---|---|
| Turbulence model | $k$-$\epsilon$ |
| Advection scheme | UDS |
| Transient model | No |
| Compressible flow model | No |

**Table 8.** Physics models selected for the last round of simulation of design point 6.

| Physics models in intelligent system(i = 5; C = 5; D = 0) | Selection |
|---|---|
| Turbulence model | RSM |
| Advection scheme | Blended scheme |
| Transient model | No |
| Compressible flow model | Yes |

Here, $\Delta p$ is calculated from the published head loss coefficient plot for flow through contracted pipe [32], $\Delta p_1$ is calculated by ANSYS CFX under the batch mode, which is a kind of routine analysis using the default setup for each design point. $\delta_1$ is the relative error between $\Delta p_1$ and $\Delta p$. Correspondingly, $\Delta p_2$ is calculated using the intelligent solver functions we put forward, and $\delta_2$ is the relative error between $\Delta p_2$ and $\Delta p$. Seen from Tab. 5, the pressure drop increases with the decreased small inner diameter. The $\delta_2$ error of the intelligent solver scheme is in the order of the uncertainty of $\Delta p$ obtained from empirical results which cannot be improved further. Analyzing the results obtained from the batch mode, the $\delta_1$ error is significantly bigger especially when much higher velocity occurs with very small $d$, which means the compressibility effect is already not negligible. In comparison, the error of the intelligent solver is 2 to 3 times smaller than the batch mode error.

The physics models selected for the batch mode are shown in Tab. 6. They remain to be unchanged during the design updating process. In the intelligent system, the changes in physics models shown in Tab. 7 and Tab. 8 respond to the compressibility effect occurs in design point 6. Hence, the reason for the difference in the error control is that the intelligent solver functions support the validation of the CFD results and the reselection of correct solver regimes if there is any validity issue. And for each design, the robust simulation model can be derived to guarantee the quality of CFD simulation results. Therefore, the CFD analysis view proposed in the paper achieves the automatic feature conversion from the design view and provides a convincible input for another view, for example, the optimization view [16], in product development process.

### 4.3. Future development outlook

As shown in Fig. 9, the loss coefficient $K_L$ is highly affected by the piping design. As the CFD analysis view we proposed is a feature-based model, the multi-way feature conversion is feasible. A potential way is to incorporate the CAE effect feature [17] which interprets the analysis results and provide the backward physical reasoning. Ideally, based on the method we proposed, an optimized

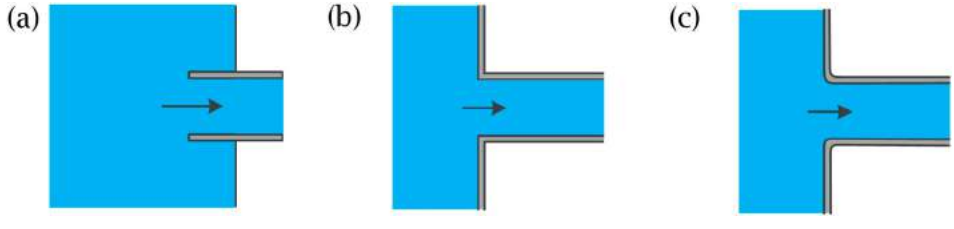


**Figure 9.** Loss coefficient in different piping design: (a) Reentrant $K_L = 0.8$, (b) Sharp-edged $K_L = 0.5$, (c) Well-rounded $K_L = 0.03 \sim 0.12$. [32]

piping design with desired loss coefficient could be developed with more cyclic CAD/CFD procedures.

The proposed intelligent CFD solver functions can be implemented based on ANSYS Workbench which provides two scripting levels. For task automation at the application level, in CFX specifically, CCL (CFX Command Language) [31] can be applied as a session to manipulate CFX-Pre and CFD-Post. Consequently, the physical rules and assisted solver functions can be executed using CCL. After the simulation is done, the post processing can be automated by CCL as well.

For task automation at the project level, Workbench scripting [31] can be used to create the whole project and invoke various applications to complete the created project. The actions performed via the GUI can be recorded as journals which are Python-based scripts. Such kind of scripts can be customized according to a specific purpose. Thus, the functions of the whole system can be greatly extended without too much scripting effort.

Based on the tools provided, the fluid physics features and dynamic physics features will be implemented by programs to edit CCL in the next step. Further, the intelligent solver functions can be fitted into a CAD/CFD integration system through Workbench scripting.

## 5. Conclusions

On top of the design view supported by the CAD fluid functional features, in this paper, the CFD analysis view is developed as a feature model to respond to the changes in the design view effectively. This CFD feature model consists of associative CAE boundary features, fluid physics features, and dynamic physics features. The feature conversion between the design view and the CFD analysis view is achieved by the CAE interface protocol. Especially, the application of fluid physics feature and dynamic physics feature enables artificial intelligence assisted solver regime selection and validation; this method leads to a robust simulation model with accurate results. The quality of the robust simulation model is guaranteed by the grid independence analysis and error estimation. The subroutine for advanced turbulence models is developed to enhance the ability of the system to model complex turbulent phenomena.

The effectiveness of the proposed method is shown by the investigation of pressure drop in a benchmark case of contracted pipe under different designs. By comparing with the empirical results, the error generated by the intelligent solver is generally 2 to 3 times smaller than that of the traditional ANSYS batch mode, which demonstrates that our proposed method has a better control over the errors as expected. It should be highlighted that the current system is established in dry steam simulation scenario. The rules used in this system are based on dry steam physical model and best practices in CFD. This approach can be applied in other contexts by adapting the relevant knowledge bases. Thus, the proposed method could provide a generic approach to integrate CFD analysis into a multiple-view product development environment.

As stated in the future development outlook, the system can be applied to optimize the piping design. The whole system will be fully implemented using CCL and Workbench scripting. Then, the robustness of the system should be validated by more complex cases. Besides, the wet steam simulation module could be developed in the future by extending the knowledge base.

## Acknowledgements

The authors would like to acknowledge Natural Sciences and Engineering Research Council of Canada (NSERC), RGL Reservoir Management, China Scholarship Council (CSC), University of Alberta and Alberta Innovates Technology Futures (AITF) for the financial support.

## ORCID

*Lei Li* http://orcid.org/0000-0002-5259-407X
*Carlos F. Lange* http://orcid.org/0000-0001-9390-8728
*Yongsheng Ma* http://orcid.org/0000-0002-6155-0167

## References

[1] Anderson, D. C.; Chang, T. C.: Geometric reasoning in feature-based design and process planning, *Computers & Graphics,* 14(2), 1990, 225–235. https://doi.org/10.1016/0097-8493(90)90034-U

[2] Bronsvoort, W. F.; Bidarra, R.; Dohmen, M.; van Holland, W.; de Kraker, K. J.: Multiple-view feature modelling and conversion, In Geometric Modeling: Theory and Practice, Springer Berlin Heidelberg, 1997, 159-174. https://doi.org/10.1007/978-3-642-60607-6_11

[3] Bronsvoort, W. F.; Jansen, F. W.: Feature modelling and conversion—key concepts to concurrent engineering, *Computers in Industry,* 21(1), 1993, 61–86. https://doi.org/10.1016/0166-3615(93)90045-3

[4] Bronsvoort, W. F.; Noort, A.: Multiple-view feature modelling for integral product development, *Computer-Aided Design,* 36(10), 2004, 929–946. https://doi.org/10.1016/j.cad.2003.09.008

[5] Cheng, Z.; Ma, Y.: Explicit function-based design modelling methodology with features, Journal of Engineering Design, 2017, 1-27. https://doi.org/10.1080/09544828.2017.1291920

[6] Cunningham, J. J.; Dixon, J. R.: Designing with features: the origin of features, In *Proceedings of the 1988 ASME International Computers in Engineering Conference and Exhibition*, 1, 1988, 237–243.

[7] Dannenhoffer, III, J. F.; Baron, J.: A hybrid expert system for complex CFD problems, In 8th Computational

Fluid Dynamics Conference, 1987, 1111. https://doi.org/10.2514/6.1987-1111

[8] de Kraker, K. J.; Dohmen, M.; Bronsvoort, W. F.: Multiple-way feature conversion to support concurrent engineering, In Proceedings of the third ACM symposium on Solid modeling and applications, 1995, 105–114. https://doi.org/10.1145/218013.218044

[9] De Martino, T.; Giannini, F.: Feature-based Product Modelling in Concurrent Engineering, In Globalization of Manufacturing in the Digital Communications Era of the 21st Century, Springer US, 1998, 351–362. http://doi.org/10.1007/978-0-387-35351-7_28

[10] Deng, Y. M.; Britton, G. A.; Lam, Y. C.; Tor, S. B.; Ma, Y.: Feature-based CAD-CAE integration model for injection-moulded product design, *International Journal of Production Research,* 40(15), 2002, 3737–3750. https://doi.org/10.1080/00207540210141643

[11] Ferziger, J. H.; Peric, M.: *Computational methods for fluid dynamics*, Springer-Verlag, Berlin etc., 2002.

[12] Hoffman, C. M.; Joan-Arinyo, R.: CAD and the product master model, *Computer-Aided Design,* 30(11), 1998, 905–918. https://doi.org/10.1016/S0010-4485(98)00047-5

[13] Hoffmann, C. M.; Joan-Arinyo, R.: Distributed maintenance of multiple product views, *Computer-Aided Design,* 32(7), 2000, 421–431. https://doi.org/10.1016/S0010-4485(00)00023-3

[14] Kutler, P.; Mehta, U.: Computational aerodynamics and artificial intelligence, In 17th Fluid Dynamics, Plasma Dynamics, and Lasers Conference, 1984, 1531. https://doi.org/10.2514/6.1984-1531

[15] Lee, R. J. V.: Information supported design for manufacture of injection-moulded rotational products, *International journal of production research,* 36(12), 1998, 3347–3366. https://doi.org/10.1080/002075498192094

[16] Li, L.; Lange, C. F.; Ma, Y.: Association of design and computational fluid dynamics simulation intent in flow control product optimization, Proceedings of the Institution of Mechanical Engineers, Part B: Journal of Engineering Manufacture, 2017, 0954405417697352. https://doi.org/10.1177/0954405417697352

[17] Li, L.; Ma, Y.: CAD/CAE associative features for cyclic fluid control effect modeling, *Computer-Aided Design and Applications,* 13(2), 2016, 208–220. https://doi.org/10.1080/16864360.2015.1084190

[18] Li, L.; Ma, Y.; Lange, C. F.: Association of Design and Simulation Intent in CAD/CFD Integration, *Procedia CIRP*, 56, 2016, 1–6. https://doi.org/10.1016/j.procir.2016.10.006

[19] Liu, J.; Ma, Y.; Fu, J.; Duke K.: A novel CACD/CAD/CAE integrated design framework for fiber-reinforced plastic parts, *Advances in Engineering Software*, 87, 2015, 13–29. https://doi.org/10.1016/j.advengsoft.2015.04.013

[20] Liu, J.; Cheng, Z.; Ma, Y.: Product design-optimization integration via associative optimization feature modeling, *Advanced Engineering Informatics,* 30(4), 2016, 713–727. https://doi.org/10.1016/j.aei.2016.09.004

[21] Ma, Y.; Tang, S. H.; Au, C. K.; Chen, J. Y.: Collaborative feature-based design via operations with a fine-grain product database, *Computers in Industry,* 60(6), 2009, 381–391. https://doi.org/10.1016/j.compind.2009.02.013

[22] Ma, Y.; Tong, T.: Associative feature modeling for concurrent engineering integration, *Computers in Industry,* 51(1), 2003, 51–71. https://doi.org/10.1016/S0166-3615(03)00025-3

[23] Rubio, G.; Valero, E.; Lanzan, S.: Computational Fluid Dynamics Expert System using Artificial Neural Networks, *World Academy of Science, Engineering and Technology, International Journal of Computer, Electrical, Automation, Control and Information Engineering*, 6(3), 2012, 413–417.

[24] Sanfilippo, E. M.; Borgo, S.: What are features? An ontology-based review of the literature, *Computer-Aided Design*, 80, 2016, 9–18. https://doi.org/10.1016/j.cad.2016.07.001

[25] Shelton, M. L.; Gregory, B. A.; Lamson, S. H.; Moses, H. L.; Doughty, R. L.; Kiss, T.: Optimization of a transonic turbine airfoil using artificial intelligence, CFD and cascade testing, In ASME 1993 International Gas Turbine and Aeroengine Congress and Exposition, American Society of Mechanical Engineers, 1993, V03AT15A012-V03AT15A012.

[26] Smit, M. S.; Bronsvoort, W. F.: Integration of design and analysis models, *Computer-Aided Design and Applications,* 6(6), 2009, 795–808. https://doi.org/10.3722/cadaps.2009.795-808

[27] Stremel, P.; Mendenhall, M.; Hegedus, M.: BPX-A Best Practices Expert System for CFD, In 45th AIAA Aerospace Sciences Meeting and Exhibit, 2007, 974. https://doi.org/10.2514/6.2007-974

[28] Suh, Y. S.; Wozny, M. J.: Interactive feature extraction for a form feature conversion system, In Proceedings of the fourth ACM symposium on Solid modeling and applications, 1997, 111-122. https://doi.org/10.1145/267734.267762

[29] Tong, S. S.: Design of aerodynamic bodies using artificial intelligence/expert system technique, In 23rd Aerospace Sciences Meeting, *American Institute of Aeronautics and Astronautics*, 14(17), 1985. https://doi.org/10.2514/6.1985-112

[30] Wesley, L. P.; Lee, J. D.; Rodman, L. C.; Childs, R. E.: Toward an integrated CFD expert system environment, In 36th AIAA Aerospace Sciences Meeting and Exhibit, American Institute of Aeronautics and Astronautics, 1998. https://doi.org/10.2514/6.1998-1005

[31] Workbench scripting Guide, ANSYS, Inc., Release 15.0, 2013, http://148.204.81.206/Ansys/150/Workbench%20Scripting%20Guide.pdf.

[32] Yunus, A. C.; Cimbala, J. M.: *Fluid mechanics fundamentals and applications*, McGraw-Hill, New York, NY, 2006.